RESEARCH PAPER

Numerical Simulation of Photocatalytic Degradation of Terbuthylazine in a Continuous Stirred Tank Reactor

Jiahao He and Baoqing Deng*

Department of Environmental Science and Engineering, University of Shanghai for Science and Technology, Shanghai 200093, P R China

Abstract
A mathematical model is presented to simulate the photocatalytic degradation of terbuthylazine in a continuous stirred tank reactor. The flow field is described by the continuity equation and the momentum equation. An advection-diffusion-reaction equation is used to simulate the transport of terbuthylazine. The chemical reactions take place on the inner wall surface coated with the catalyst, which is described by a third-kind boundary condition. A transient differential equation is used to describe the variation of inlet concentration with time. All governing equations are solved using the commercial computational fluid software ANSYS Fluent. The simulation results agree with the experimental data at different temperatures and different flow rates. The radial distribution of terbuthylazine in the reactor is discussed in detail. The velocity depicts a parabolic curve with a maximum velocity of 0.0005 m s^{-1}, 0.001 m s-1, 0.00022 m s^{-1} and 0.0032 m s^{-1} for 50 mL min^{-1}, 100 mL min^{-1}, 200 mL min^{-1}, and 300 mL min^{-1}, respectively. At the flow rate of 300 mL min^{-1}, concentration of terbuthylazine decreases from 3.6 mg dm^{-3} to 0.8 mg dm^{-3} whereas concentration of cyanuric acid increases from 0.05 mg dm^{-3} to 0.28 mg dm^{-3}. It shows that the radial effect of velocity and concentration should be taken into account. The mathematical model used in this study is suitable for simulating the photocatalytic degradation process of terbuthylazine in continuous stirred tank reactors.

Keywords: Terbuthylazine; Continuous stirred-tank reactors; Photocatalytic degradation; Computational fluid dynamics

INTRODUCTION

Persistent organic pollutants have been identified as endocrine disrupting chemicals, which is recalcitrant toward remediation and toxic to microorganisms (Tang et al. 2019; Botta et al. 2002). Since conventional degradation methods are not effective in degrading persistent organic pollutants. Advanced oxidation processes are gaining increasing interest (Rizzo 2011; Malato et al. 2009; Avasarala et al. 2011; Chen et al. 2009; Ayati et al. 2014). As a popular advanced oxidation technology, photocatalytic oxidation technology can oxidize pollutants into carbon dioxide and water. The reaction kinetics of photocatalytic oxidation is concerned with the catalyst, UV light, etc and requires to be experimentally determined.

Continuous stirred-tank reactors (CSTR) system is a closed pipeline with a stirred tank and a photocatalytic reactor. The fluid leaves the stirred tank, enters the photocatalytic reactor, and re-enters the stirred tank. The stirred tank ensures the good mixing of fluid without reaction whereas the reaction only takes place in photocatalytic reactors. Computational fluid dynamics (CFD) have been widely used to optimize the performance of CSTR. Sommer and Kirchen

---

* Corresponding author Email: bqdeng@usst.edu.cn

(2019) presented a simplified computationally inexpensive, coupled, two-chamber CSTR model to investigate the improvement of partial oxidation product. A number of reactor parameters were efficiently identified by using the two-chamber CSTR model. Calder´on and Ancheyta (2018) simulated the conversion process of heavy oil in CSTR to find the best working conditions improving the conversion rate of reactants. Cao et al. (2020) described a computationally efficient simulation of heavy-residue gasifiers and validated the model against industrial data. Srirugsa et al. (2017) explained the mixing characteristics and hydrogen production of turbine by using the CFD simulation. Ri et al. (2019) simulated the degradation of ethanol in horizontal continuous stirred tank reactor and vertical continuous stirred tank reactor, analyzed the effect of hydraulic retention time on hydrogen production, and determined the optimal hydrogen production conditions of horizontal continuous stirred tank reactor. When using CFD to optimize reactors, the reaction kinetics should be offered.

Continuous stirred-tank reactors can also be used to measure the reaction kinetics (Jeppu et al. 2012). By monitoring the variation of concentration of pollutants with time, the reaction kinetics can be derived (Roudsari et al. 2013; Lefebvre et al. 2018; Kanaujiya and Pakshirajan 2022; Tsapekos et al. 2018; Salmi et al. 2022; Cheng 2020). These studies neglect flow field and distribution of substrates in the reactor. In the present study, a CFD model is presented to simulate the distribution of substrates in CSTR and discuss the effect of flowfield on the reaction kinetics. The effect of temperature on the reaction kinetics is also studied in detail.

MATERIALS AND METHODS
Physical model
Experiemnts of photocatalytic degradation were conducted in a batch recirculating photocatalytic device (Le Cunff et al. 2018). The photocatalyst was placed near the inner side of the outside wall of reactor. A peristaltic pump was used to recirculate the solution with different flow rate. The computational domain is shown in Figure 1. The total length of the reactor is 30 cm. The inner diameter of the tube is 6 cm. The inner tube is a movable quartz test tube with an outer diameter of 2.5 cm. A HNS G5 germicidal lamp is placed in the quartz tube with a power of 8 W. The lamp tube is located in the center of the quartz tube, and the catalyst is immobilized titanium dioxide. The reactants enter the reaction system from the inlet on the left side of the reactor for photocatalytic reaction, and the reaction residues and reaction products flow out from the outlet on the right side of the reactor. Concentrations of terbuthylazine and cyanuric aciddegradation were identified using LC/MS.

Governing equations
When the CSTR system operates steadily, the flow in the CSTR system is steady. Thus, the flow in the photocatalytic reactor can be described by the continuity equation and the momentum equation as follows

$$\frac{\partial u_j}{\partial x_j} = 0 \tag{1}$$

$$\frac{\partial}{\partial x_j}\left(\rho u_i u_j\right) = \frac{-\partial p}{\partial x_i} + \frac{\partial}{\partial x_j}\left(\mu \frac{\partial u_i}{\partial x_j}\right) \tag{2}$$

where ρ is the fluid density, t is the time, x_j is the coordinate component, u_j is the velocity component, p is the pressure, μ is the dynamic viscosity.

The reaction takes place in the photocatalytic reactor either in the reactor volume or at the
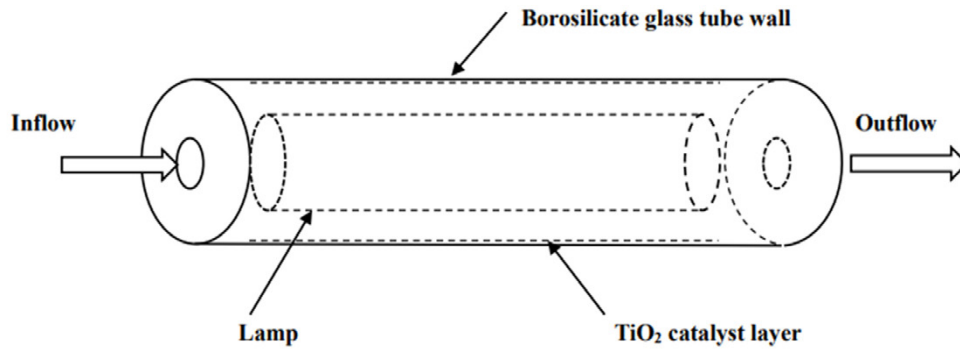
Fig. 1. Schematic diagram of CSTR model

wall of reactor. Thus, the concentration in the CSTR varies with time. The concentration of pollutants in the photocatalytic reactor should be described by a transient advection-diffusion equation as follows

$$\frac{\partial C}{\partial t} + \frac{\partial}{\partial x_j}\left(u_j C\right) = \frac{\partial}{\partial x_j}\left(D\frac{\partial C}{\partial x_j}\right) \tag{3}$$

where, C is the concentration of pollutants, D is the diffusion coefficient of pollutants, σ_t is the turbulent Schmidt number.

Boundary conditions
At the inlet, the velocity is specified. Since the concentration of pollutants varies with time, a time-dependent condition should be defined

$$V\frac{dC_i}{dt} = C_o Q - C_i Q \tag{4}$$

V is the volume of stirred tank, C_i is the concentration at the inlet of the photocatalytic reactor, C_o is the concentration at the outlet of photocatalytic reactor, and Q is the circulating flowrate. At the outlet, fully developed flow is assumed.
At all walls, no-slip condition is applied for flow. For walls without reaction, pollutants meet

$$\frac{\partial C}{\partial n} = 0 \tag{5}$$

For walls with reaction, pollutants meet

$$-D\frac{\partial C}{\partial n} = r \tag{6}$$

where, r is the rate of reaction on the surface of the catalyst.
In the photocatalytic reactor, terbuthylazine may undergo a series of complex chemical reactions, the final product is cyanuric acid, CO_2, NH_3, and some intermediate products will
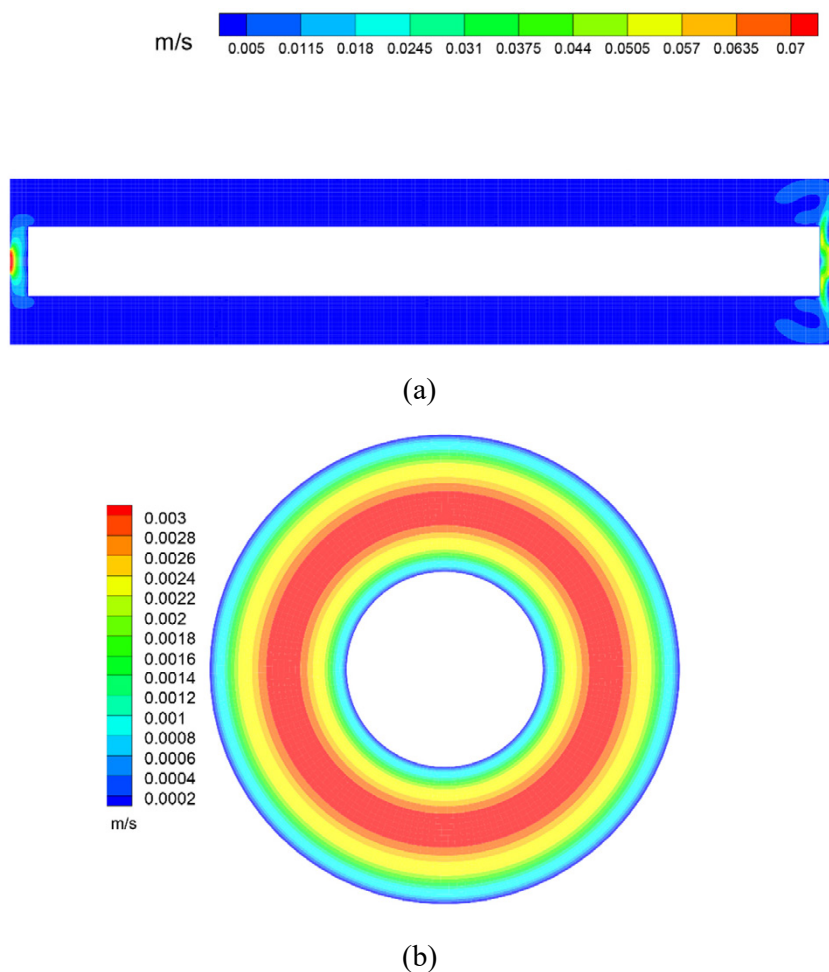
(a)

(b)

Fig. 2. The distribution of velocity at $x = -0.15$ m for the flow rate of 300 cm³ min⁻¹

be produced in the reaction. Le Cunff et al. (2018) proposed that terbuthylazine reacted with oxygen, becoming cyanuric acid through the intermediate product. Thus, the reaction kinetics can be written as follows

$$r_{TBA} = \rho k_1 C_{TBA}^n \tag{7}$$

$$r_M = \rho k_1 C_{TBA}^n - \rho_c k_2 C_M^n \tag{8}$$

$$r_{CYA} = \rho k_2 C_M \tag{9}$$

where, r_{TBA} is the degradation rate of terbuthylazine, r_M is the degradation rate of the intermediate product, r_{CYA} is the generation rate of cyanuric acid, ρ is the density of the catalyst, where the value of n is 1.5, k_1 and k_2 are the reaction rate constants.
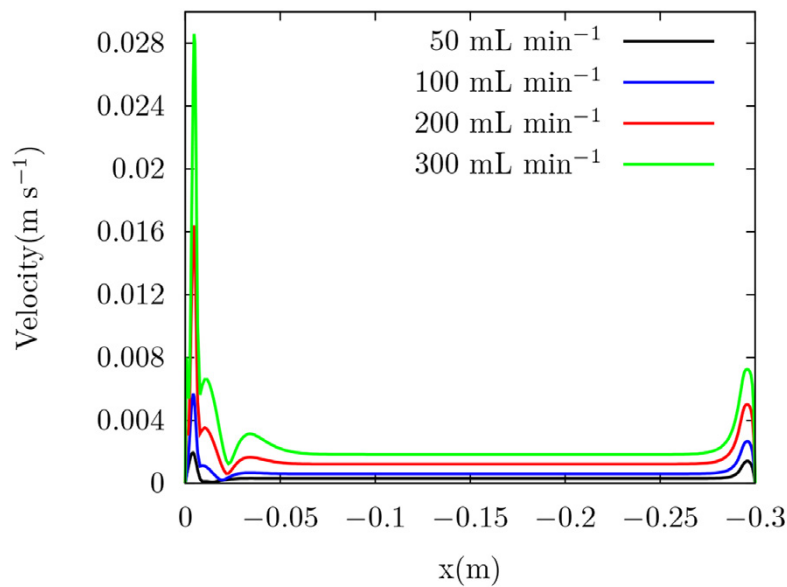
Computational procedure
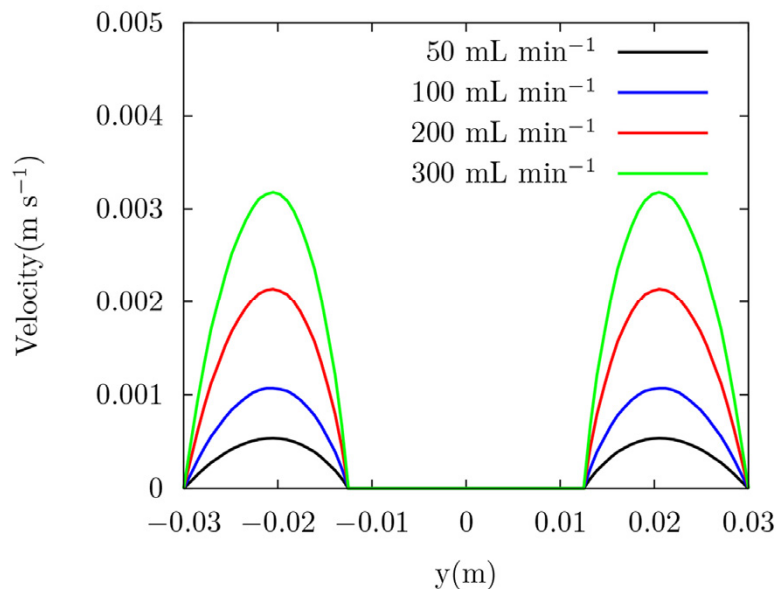   Hexahedral mesh is used to discretize the computational domain. The total number of

meshes is about 1.04 million. ANSYS Fluent is used to solve governing equations. The pressure-velocity coupling is treated using the SIMPLE algorithm. All convection terms are discretized with second-order upwind differencing scheme. When the residuals for all equations except concentration are less than 1.0×10^{-4}, the computation is assumed convergent.

RESULTS AND DISCUSSION

Figure 2 shows the distribution of velocity at $x = -0.15$ m for the flow rate of 300 $cm^3 min^{-1}$.

a) y=0.025m,z=0m

(b) $x = -0.15$ m, $z = 0$ m

Fig. 3. Velocity along the radial direction

(a) Terbuthylazine

(b) Cyanuric acid

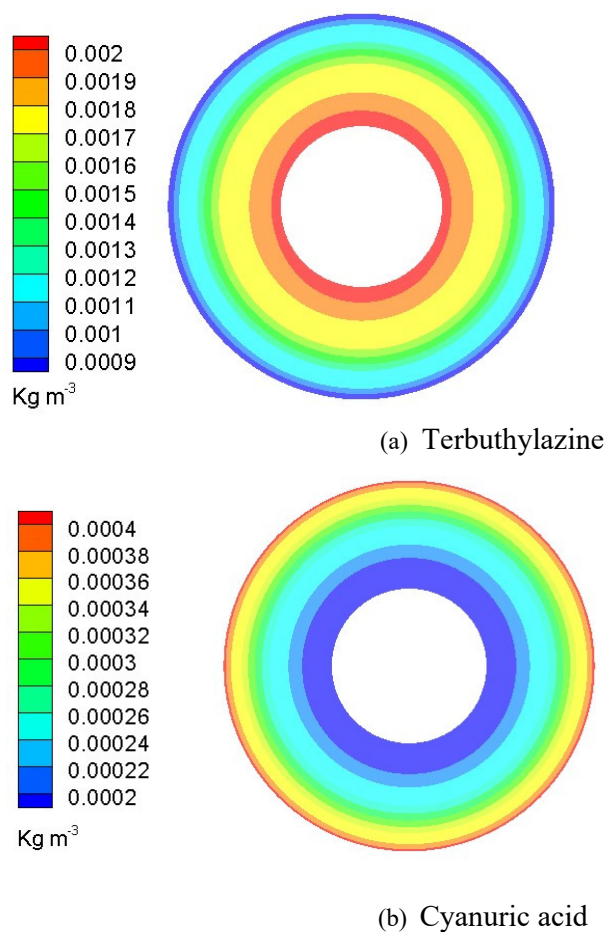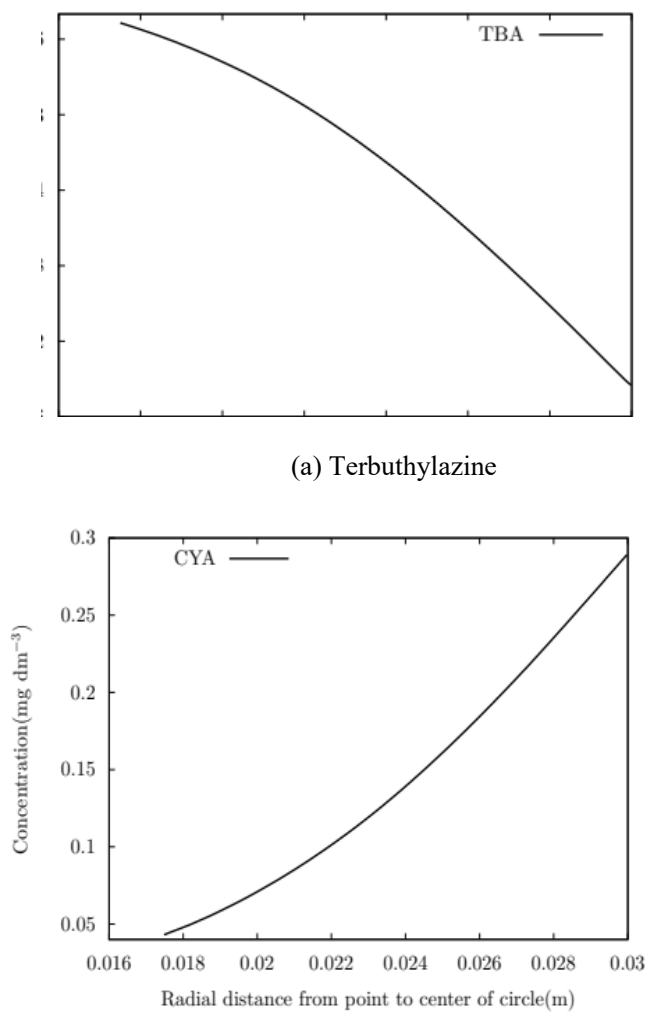**Fig. 4.** Concentration at x = -0.15 m at 300 cm^3 min^{-1} flow rate

In the reactor, there are high velocity zones near the inlet and outlet. The flow pattern is typical of channel flow with high velocity in the center of the channel. Figure 3 shows the velocity component in x direction at the position of $x = -0.15$ m, $z = 0$ m. It can be seen from the figure that the maximum velocity at the center of the pipe in the CSTR can reach 0.032 ms^{-1}, which is about twice the average velocity. It can be seen from the figure that the fluid has the highest velocity at the center between the catalytic layer and the lamp tube. The closer it is to the tube wall, the lower the velocity.

Figure 4 illustrates the concentration distribution of reactant terbuthylazine and product cyanuric acid in the reactor. The concentration of terbuthylazine near the TiO$_2$ catalyst layer is the lowest since it is oxidized into the product. The pattern for the product cyanuric acid is on the contrary because it is produced on the catalyst layer.
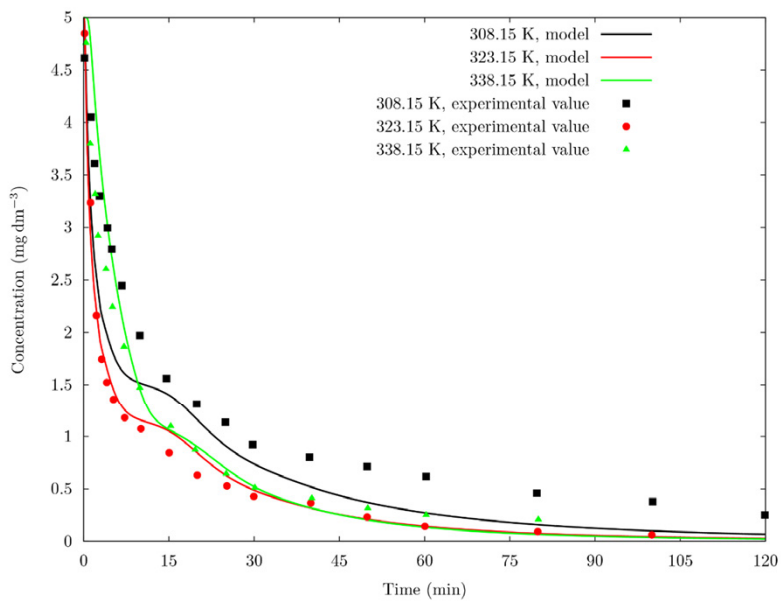
Figure 5 shows the radial concentration distribution of reactant terbuthylazine and product cyanuric acid at the position of (x =-0.15 m, y = 0.0125 m) at $t = 10$ min. A non-uniform distribution is observed for two concentrations. The concentration of terbuthylazine is higher near the lamp tube wall and lower near the reactor wall. This is because the catalyst is located on the inner wall of the reactor, where the catalytic reaction degrades terbuthylazine. It means that one dimensional simulation of CSTR may not reproduce the distribution of pollutants in the reactor and thus may have effect on the solution of kinetic equation of pollutant degradation.

Le Cunff et al. (2018) measured the concentration of terbuthylazine and cyanuric acid at different temperature and flow rate. The concentration of terbuthylazine decreased with the

(a) Terbuthylazine

(b) cyanuric acid

Fig. 5. Variation of concentration along radius at a flow rate of 300 cm^3 min^{-1}

Fig. 6. Comparison of model and experimental values of terbuthylazine concentration at different temperature

increasing time. On contrary, the concentration of cyanuric acid increased with the increasing time. These experimental curves are used to validate the present model.

Figure 6 shows the consumption of terbuthylazine with time under different temperatures. A similar pattern can be observed for three temperatures. When the temperature is 308.15 K, the terbuthylazine concentration decreases from the initial value of 5 mg dm^{-3} to 1.40 mg dm^{-3} during 15 minutes. After 15 min, terbuthylazine concentration decreased gradually. The growth rate of product cyanuric acid concentration is relatively stable. At 323.15 K, the degradation rate of terbuthylazine was the fastest in the first 15 minutes, especially in the initial two minutes. When the reactor was run for 15 min, the concentration of terbuthylazine degraded to less than 1 mg dm^{-3}. Figure 7 show the production of cyanuric acid with time under different temperatures. When the temperature is 308.15 K, the final concentration of cyanuric acid is 2.2 mg dm^{-3}; When the temperature was 323.15 K, the final concentration of cyanuric acid was 2.4 mg dm^{-3}; When the temperature was 338.15 K, the final concentration of cyanuric acid was 2.5 mg dm^{-3}. The concentration of cyanuric acid increases with the increase of temperature. This is because the reaction temperature has a significant effect on the degradation of some intermediates, resulting in different main degradation pathways, and ultimately affect the formation of cyanuric acid.

Figure 8 and 9 depict the effect of flow rate on the reaction. When the temperature is 298.15 K. In the first 30 minutes, the degradation rate of terbuthylazine is the fastest, and after 30 minutes, the degradation rate curve of terbuthylazine tends to be stable. Figure 8 show that when the recirculation rate is 50 cm^3 min^{-1}, the concentration of terbuthylazine in the first 30 minutes drops from the initial 5 mg dm^{-3} to 0.22 mg dm^{-3}. When the flow rate was 100 cm^3 min^{-1}, 200 cm^3 min^{-1}, and 300 cm^3 min^{-1}, the concentration of terbuthylazine in the first 30 minutes decreased by 4.63 mg dm^{-3}, 4.33 mg dm^{-3}, and 4.26 mg dm^{-3}, respectively.
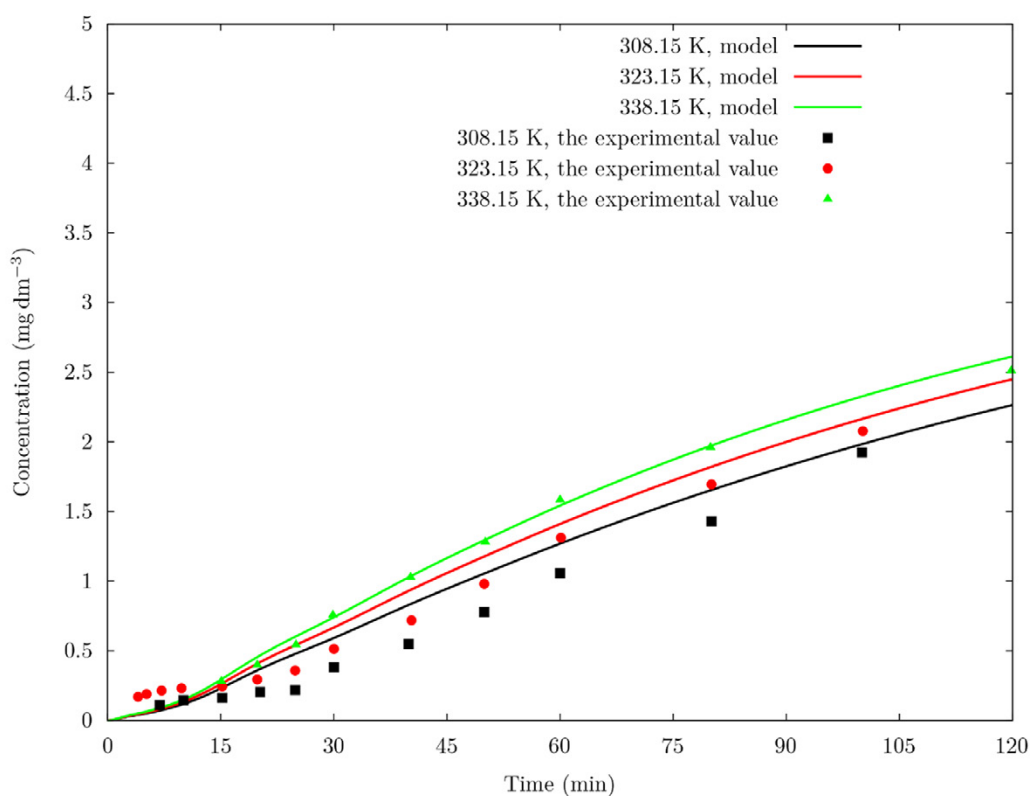

Fig. 7. Comparison of model and experimental values of cyanuric acid concentration at different temperature
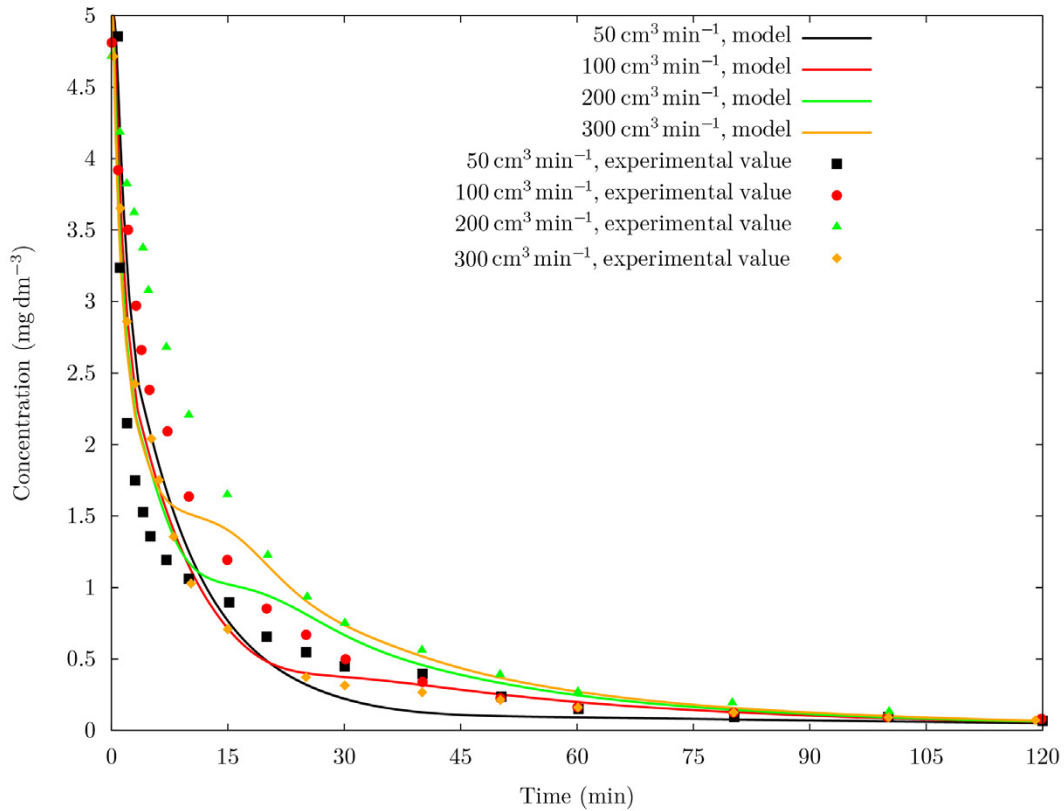
Fig. 8. Comparison of model and experimental values of terbuthylazine concentration at different flow rates
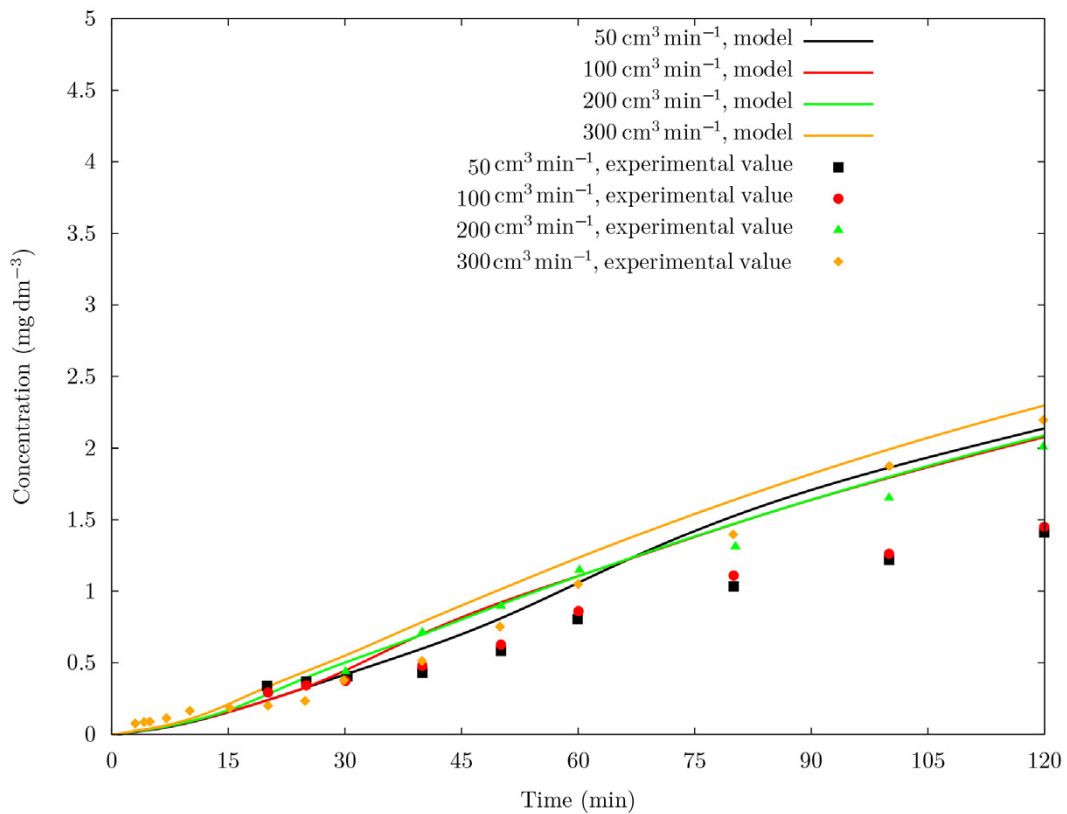

Fig. 9. Comparison of model and experimental values of cyanuric acid concentration at different flow rates

CONCLUSION

The modeling of photocatalytic degradation of terbuthylazine at different temperatures and flow rates in CSTR is studied using CFD. The computed results confirmed the accuracy of CFD model in predicting the behavior of the CSTR. The reaction kinetics of the model incorporates a terbuthylazine kinetics for chemical reactions.

In the radial direction, terbutrazine concentration near the outer wall of CSTR is the lowest and cyanuric acid concentration is the highest; The terbuthylazine concentration near the quartz tube is the highest and the cyanuric acid concentration is the lowest, which is consistent with the coating of catalyst on the outer wall of the reactor. The CFD modeling results agree well with the experimental data in terms of the temperature and flow rate in terms of the terbuthylazine degradation. The results showed that temperature has no significant effect on the degradation of terbuthylazine, but has a great effect on the formation of cyanuric acid. This is because the temperature has a great impact on some intermediate products and finally affects the formation of cyanuric acid.

GRANT SUPPORT DETAILS

CONFLICT OF INTEREST

The authors declare that there is not any conflict of interests regarding the publication of this manuscript. In addition, the ethical issues, including plagiarism, informed consent, misconduct, data fabrication and/ or falsification, double publication and/or submission, and redundancy has been completely observed by the authors.

LIFE SCIENCE REPORTING

No life science threat was practiced in this research.

REFERENCES

Avasarala, B. K., Tirukkovalluri, S. R. and Bojja, S. (2011). Photocatalytic degradation of monocrotophos pesticide—an endocrine disruptor by magnesium doped titania. *Journal of hazardous materials*,186 (2-3),1234–1240.

Ayati, A., Ahmadpour, A., Bamoharram, F. F., Tanhaei, B., M¨antt¨ari, M. and Sillanp¨a¨a, M. (2014). A review on catalytic applications of Au/TiO2 nanoparticles in the removal of water pollutant. *Chemosphere*,107,163–174.

Botta, S. G., Rodr´ıguez, D. J., Leyva, A. G. and Litter, M. I. (2002). Features of the transformation of HgII by heterogeneous photocatalysis over TiO2. *Catalysis today*,76 (2-4),247–258.

Calder´on, C. J. and Ancheyta, J. (2018). Modeling of CSTR and SPR small-scale isothermal reactors for heavy oil hydrocracking and hydrotreating. *Fuel*,216,852–860.

Cao, Z., Wu, Q., Zhou, H., Chen, P. and You, F. (2020). Dynamic modeling, systematic analysis, and operation optimization for shell entrained-flow heavy residue gasifier. *Energy*,197,117220.

Chen, C., Yang, S., Guo, Y., Sun, C., Gu, C. and Xu, B. (2009). Photolytic destruction of endocrine disruptor atrazine in aqueous solution under UV irradiation: products and pathways. *Journal of hazardous materials*,172 (2-3),675–684.

Cheng, K.-C. (2020). Kinetic model of hyperbranched polymers formed by self-condensing vinyl polymerization of inimers and trifunctional cores with different reactivities in a continuous-stirred tank reactor. *Chemical Engineering and Processing - Process Intensification*,147,107739.

Jeppu, G. P., Clement, T. P., Barnett, M. O. and Lee, K.-K. (2012). A modified batch reactor system to study equilibrium-reactive transport problems. *Journal of contaminant hydrology*,129,2–9.

Kanaujiya, D. K. and Pakshirajan, K. (2022). Mass balance and kinetics of biodegradation of endocrine disrupting phthalates by Cellulosimicrobium funkei in a continuous stirred tank reactor system. *Bioresource Technology*,344,126172.

Le Cunff, J., Tomaˇsi´c, V. and Gomzi, Z. (2018). Photocatalytic degradation of terbuthylazine: Modelling of a batch recirculating device. *Journal of Photochemistry and Photobiology A: Chemistry*,353,159–170.

Lefebvre, J., Trudel, N., Bajohr, S. and Kolb, T. (2018). A study on three-phase CO2 methanation reaction kinetics in a continuous stirred-tank slurry reactor. *Fuel*,217,151–159.

Malato, S., Fern´andez-Ib´an˜ez, P., Maldonado, M. I., Blanco, J. and Gernjak, W. (2009). Decontamination and disinfection of water by solar photocatalysis: recent overview and trends. *Catalysis today*,147 (1),1–59.

Ri, P.-C., Kim, J.-S., Kim, T.-R., Pang, C.-H., Mun, H.-G., Pak, G.-C. and Ren, N.-Q. (2019). Effect of hydraulic retention time on the hydrogen production in a horizontal and vertical continuous stirred-tank reactor. *International Journal of Hydrogen Energy*,44 (33),17742–17749.

Rizzo, L. (2011). Bioassays as a tool for evaluating advanced oxidation processes in water and wastewater treatment. *Water research*,45 (15),4311–4340.

Roudsari, S. F., Ein-Mozaffari, F. and Dhib, R. (2013). Use of CFD in modeling MMA solution polymerization in a CSTR. *Chemical engineering journal*,219,429–442.

Salmi, T., Tolvanen, P., Er¨anen, K., W¨arn˚a, J., Leveneur, S. and Haario, H. (2022). Determination of kinetic constants by using transient temperature data from continuous stirred tank reactors. *Chemical Engineering Science*,248,117164.

Sommer, D. E. and Kirchen, P. (2019). Towards improved partial oxidation product yield in mixed ionic-electronic membrane reactors using CSTR and CFD modelling. *Chemical Engineering Science*,195,11–22.

Srirugsa, T., Prasertsan, S., Theppaya, T., Leevijit, T. and Prasertsan, P. (2017). Comparative study of Rushton and paddle turbines performance for biohydrogen production from palm oil mill effluent in a continuous stirred tank reactor under thermophilic condition. *Chemical Engineering Science*,174,354–364.

Tang, J., Chen, Y. and Dong, Z. (2019). Effect of crystalline structure on terbuthylazine degradation by H2O2-assisted TiO2 photocatalysis under visible irradiation. *Journal of Environmental Sciences*,79,153–160.

Tsapekos, P., Kougias, P. G., Kuthiala, S. and Angelidaki, I. (2018). Co-digestion and model simulations of source separated municipal organic waste with cattle manure under batch and continuously stirred tank reactors. *Energy Conversion and Management*,159,1–6.